



## Research Article

# Electric Cell-Substrate Impedance Sensing (ECIS) for Analyzing the Effect of Environmental Pollutants - A Study of Diesel Exhaust Nanoparticles

Amalu Navas<sup>1</sup>, Maya Nandkumar A<sup>2\*</sup>

<sup>1</sup>PhD Scholar, Division of Microbial Technology, BMT Wing, SCTIMST, Poojappura, Thiruvananthapuram, Kerala, India

<sup>2</sup>Scientist 'G' and Head, Division of Microbial Technology, BMT Wing, Sree Chitra Tirunal Institute for Medical Sciences and Technology, Thiruvananthapuram-12, Kerala, India

\***Corresponding Author:** Dr A Maya Nandkumar, Scientist 'G' and Head, Division of Microbial Technology, BMT Wing, SCTIMST, Poojappura, Thiruvananthapuram, Kerala, India

**Received:** 11 May 2022; **Accepted:** 18 May 2022; **Published:** 26 May 2022

**Citation:** Amalu Navas, Maya Nandkumar A. Electric Cell-Substrate Impedance Sensing (ECIS) for Analyzing the Effect of Environmental Pollutants - A Study of Diesel Exhaust Nanoparticles. Journal of Environmental Science and Public Health 6 (2022): 189-203.

### Abstract

ECIS is a morphological biosensor that records the electrical properties of cell-covered microelectrodes in an AC circuit, including impedance (ohm), resistance (ohm), and capacitance ( $\mu$ Farad). The objective of the current study was to analyze the suitability of ECIS as a label-free *in vitro* assay system to understand the effect of external stimuli on cells in real-time, vis-à-vis regular endpoint assays of cytotoxicity. The study analyzed whether fluctuations

in the electrical properties of cell-covered microelectrodes reflected dynamic changes in cell morphology on exposure to diesel exhaust particles. Exposure of A549 monolayers in 8 well microarrays to DEP caused significant changes in microelectrode resistance (ohm @4 kHz) as compared to controls within 24 h. Variations in impedance were found to have a dose-dependent effect. We compared our results from ECIS with classic cytotoxicity analyses

like MTT, LDH, and NRU assays and observed corroborative endpoint results. Reactive oxygen species production by DCFHDA assay showed an increase in relative fluorescence indicating ROS to be a possible cause of dose-dependent cytotoxicity.

Our findings indicate that ECIS provides many benefits as an alternative method to quantify, automate, and measure the effect of pollutants or particles in real-time when compared to traditional endpoint methods.

**Keywords:** ECIS; Diesel exhaust nanoparticles; Cytotoxicity; Label-free; Real-time

## 1. Introduction

Electric cell-substrate impedance sensing (ECIS) is a real-time label-free method for analyzing cellular behavior to an external injury or stimuli using in vitro cell cultures. The system measures changes in impedance/resistance in cell monolayers in real-time and thus provides information faster vis-à-vis endpoint or labelled assays. Most conventional analyses are invasive, use multiple labels, are labor-intensive and provide only endpoint results. Examples of label-free methods include techniques like optical light spectroscopy, quartz microbalance, and electric cell-substrate impedance sensing (ECIS). Among them, ECIS is a powerful tool to assess cellular properties and physiology. This method has attracted wide attention as it overcomes the limitations of conventional endpoint analyses. Ever since Giaever and Keese (1984) invention, ECIS has been used to monitor cell motion, attachment, and spreading and assess cell migration in wound healing assays [1].

In ECIS cells are grown in arrays with golden electrodes at the bottom. A small alternating current (AC) is applied across electrodes patterned at the bottom of arrays, resulting in potential differences across electrodes measured by the ECIS instrument. As cells attach to electrodes and proliferate, resistance increases to the current flow corresponding to morphology and the number of cells covering the electrode. The results are plotted as an impedance versus time graph.

AC frequencies are important in ECIS. Current flow always takes a path of low resistance. At low frequencies, membrane impedance is higher, so most of the current flows in the solution channels under and between cells, whereas at higher frequencies (>40,000Hz) current flows mostly through the insulating cell membranes. Thus, high-frequency impedance is affected by cell coverage and give details about cell spreading and establishment of confluent layer and low frequency will give details about barrier integrity. In the more advanced Z $\theta$  equipment, the impedance will be broken down to resistance and capacitance, allowing for more accurate data of the cell behavior, making it an advanced form of cellular impedance-based assays.

Air pollution has been linked to increased morbidity and mortality of pulmonary diseases. Exposure to airborne particulate matter has a strong correlation with adverse outcomes like reduced lung function, premature death [2, 3, 4]. Diesel exhaust nanoparticles (DEP) are a major component of particulate matter in air pollution. DEP results from incomplete combustion of diesel fuel. It is composed of a central core of elemental carbon and adsorbed

organic compounds including Polyaromatic hydrocarbons (PAHs) and nitro-PAHs, and small amounts of sulfate, nitrate, metals, and other trace elements [5] differing in composition depending on the source of collection. These particles having large surface area are highly respirable and are in the nanosize range, reaching the deep portions of the lungs -like the gas exchange regions or alveoli. Airway epithelial cells form an innate line of defense to inhaled allergens, particulates, and pathogens, affected through a combination of secreted mucus and apical junctional complexes (AJC). Our study demonstrates ECIS as an effective tool to understand the effect of nano aerosolized pollutants on the alveolar epithelial cells vis-à-vis regular endpoint analysis.

## 2. Materials and Method

### 2.1 Cell culture

Kaighn's modification of Ham's F12 (F12K), Trypsin EDTA, Gentamycin, Amphotericin B solutions were purchased from Hi-media Pvt. Ltd. (Mumbai, India). Fetal bovine serum (FBS) was purchased from Gibco (Grand Island, NY, USA). 3-(4,5-Dimethylthiazol-2-yl)- 2,5-diphenyltetrazolium bromide (MTT), trypan blue, Neutral red dye was purchased from Sigma Chemicals Co. Ltd. (St. Louis, MO, USA). LDH assay was done by using CytoTox96® Non-Radioactive Cytotoxicity Assay kit from Promega. DCFHDA was purchased from Thermo fisher scientific (Waltham, Massachusetts).

### 2.2 Diesel exhaust nanoparticle preparation and characterization

The diesel exhaust particles (DEP) were collected from a diesel car engine exhaust. The exhaust

particles were collected into a membrane filter made of cellulose ester as total suspended particulates. Particles were collected by sonicating the filter for 45mins in 5ml of ultrapure water using a bath sonicator. The suspension was then centrifuged at 10,000rpm for 15mins and lyophilized (Lyolab). Stock solution of diesel exhaust nanoparticles was prepared in complete cell culture medium and sonicated prior to exposure. This was used as DEP in the study. DEP was characterized by Transmission electron microscopy. (JEOL JEM TEM).

### 2.3 Impedance measurement with ECIS

ECIS was used to study the effect of diesel exhaust particles in A549 cells. The array type used was 8W10E+ (Applied Biophysics, NY, USA), consisting of eight wells, each with two sets of 20 circular active electrodes with 250 µm diameter located on inter-digited fingers to provide measurements upon 40 electrodes in total. Each well has a substrate area of 0.8cm<sup>2</sup> and volume of 600 µL.

The 10E+ arrays used for the study were designed to monitor a large number of cells, sampling over the entire bottom of the well. Arrays were attached to the ECIS system (Model ECIS Z0, Applied Biophysics, NY, USA), and alternative current (I) of 4000 Hz was applied to the sensing electrodes. Low frequencies were used to assess cellular barrier function, as at higher frequencies, current flows capacitively through the cell membrane, whereas at low frequencies, the membrane impedance increases, and current flows through the cellular junctions, which offer lesser resistance (Figure 1).

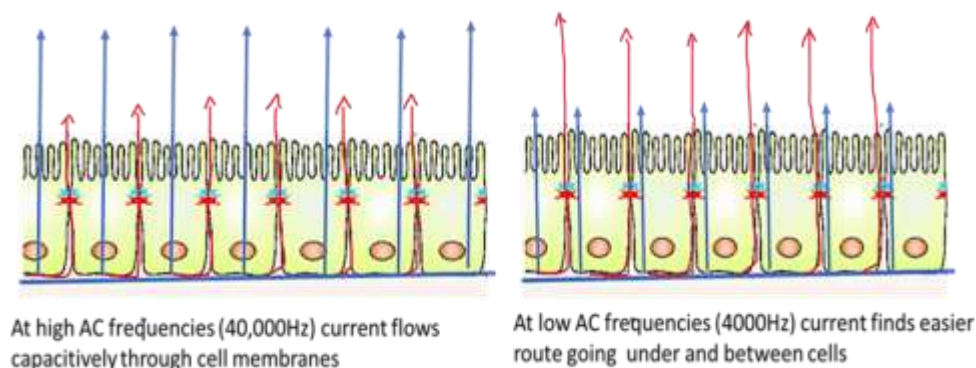


**Figure 1:** Is a pictogram depicting the cross-section of a confluent cell monolayer inside the ECIS well array and the probable path of current flow at different frequencies is indicated by the arrows.

Prior to the experiment, the array holder was warmed to 37°C in the incubator [6]. Before seeding the cells, 400µl of complete cell culture medium was added to the 8Well. The arrays were placed on the array holder, such that the gold-plated electrode pads were aligned with the spring-loaded pogo pins and the screws were tightened. The connectivity and impedance were checked. After stabilization of electrodes cell-free impedance was measured. After 1hr the impedance measurement was paused and arrays were removed. The media in the wells were replaced with fresh F12K medium. A549 cells were seeded at a density of  $10^4$  cells/electrode. The electrodes were placed on the array holder, the connectivity to each well was checked and impedance measurement resumed. As the cells adhered and spread on the electrode, the impedance increased. Once complete electrode coverage was attained by the formation of a monolayer, the impedance measurement plateaued.

**2.3.1 Post- exposure measurement:** Impedance measurement was carried out till confluence by the method as previously described. Following

confluence, impedance measurement was paused and the medium in the wells was replaced by DEP in F12K medium was added in varying concentrations. The impedance measurement was continued for the duration of the experiment. The data was analyzed using Z0 ECIS analysis software. After normalization, the data was plotted against time.

## 2.4 Classic cytotoxicity analyses

**2.4.1 Assessment of cell viability:** The MTT assay, assesses metabolic reduction of 3-(4,5-dimethylthiazol-2-yl)-2,5-diphenyl-tetrazolium bromide reagent to formazan crystals. In brief, A549 cells ( $1 \times 10^4$ ) were seeded into each well of a 96 well plate. Cells were treated with different concentrations of DEP (1, 10, 20, 40, 80, 160, 320 µgm/ml) for 24 h. Following exposure, the medium was removed and cells were washed with PBS. 50 µg/well MTT solution in PBS was added to the wells and incubated for 4hrs. Precipitated formazan crystals were dissolved with 100µl DMSO. Absorbance was read at 540 nm (Bio-Tek Instruments Inc). The percentage of cell viability was calculated as

Viability% =  $\frac{A_{\text{exp}} - A_{\text{bl}}}{A_{\text{con}} - A_{\text{bl}}} \times 100$  where  $A_{\text{exp}}$  is the absorbance of the experimental group,  $A_{\text{bl}}$  is the absorbance of the blank group, and  $A_{\text{con}}$  is the absorbance of the control group.

#### 2.4.2 Assessment of plasma membrane integrity by

##### **lactate dehydrogenase assay (LDH):**

LDH assay helps in plasma membrane integrity assessment by evaluating released Lactate dehydrogenase. In brief,  $1 \times 10^4$  cells were seeded into each well of a 96 well plate. Cells were treated with different concentrations of DEP (1, 10, 20, 40, 80, 160, 320  $\mu\text{g}/\text{ml}$ ) for 24 h. One set of cells treated with complete lysis solution for 45 mins served as cell control for maximum LDH release. 50  $\mu\text{l}$  of culture supernatant from all wells were transferred to a new 96 well plate. 50  $\mu\text{l}$  of enzyme-substrate solution was added to each well and incubated for 30 mins. LDH was assessed using Promega cytotox96 @non-radioactive kit. Stop Solution was added, and the absorbance signals were measured at 490nm.

#### 2.4.3 Lysosomal integrity by Neutral red uptake

##### **assay:**

Neutral red assay measures the lysosome integrity based on the vital dye Neutral red uptake by live cells. Borenfreund and Puerner [7] originally developed this simple and accurate method. Cells were seeded in a 96 well plate with a density of  $1 \times 10^4$  cells/well and incubated at  $37^\circ\text{C}$  overnight. Meanwhile, 1% neutral red reagent was also prepared and incubated separately at  $37^\circ\text{C}$  overnight. Next day, A549 cells were treated with different concentration of DEP 1, 10, 20, 40, 80, 160, 320  $\mu\text{g}/\text{ml}$  for 24h. After treatment, 10  $\mu\text{l}$  of 1% neutral red was added to each well and incubated for 3 h at  $37^\circ\text{C}$  with 5%  $\text{CO}_2$ . At the end of the incubation period, dye was removed

and the wells were washed with PBS. The dye entrapped inside the cell was solubilized using acid alcohol desorbing agent (1% glacial acetic acid and 90% ethanol, and V/V) and the plates were incubated in dark for 30 min. Absorbance was read spectrophotometrically at 540 nm in a microplate reader.

#### 2.5 Assessment of mechanism of cytotoxicity

##### **2.5.1 Intracellular reactive oxygen species (ROS)**

##### **generation assessment by DCFH-DA:**

The production of intracellular ROS was determined by DCFH-DA (Dichloro dihydro fluorescein diacetate), a fluorometric probe that passively enters the cell. The resultant compound dichlorofluorescein (DCF) formed from reaction with intracellular ROS is highly fluorescent. For the assay, cells were seeded at a density of  $1 \times 10^4$  cells/well and cultured for 24 h. Cells were exposed to different concentration of DEP (1, 10, 20, 40, 80, 160, 320  $\mu\text{g}/\text{ml}$ ) and ROS was assessed after 3hrs and 24hrs. 0.09% hydrogen peroxide ( $\text{H}_2\text{O}_2$ ) treated cells were used as the positive control (pc). Untreated cells served as negative control. After treatment, cells were washed with PBS and incubated with 100  $\mu\text{l}$  of DCFH-DA (1 $\mu\text{M}$ ) for 45 min in dark and excess DCFH-DA was removed and replaced with 200 $\mu\text{l}$  PBS. Fluorescence was measured using a microplate reader (Synergy Biotek) with excitation and emission at wavelength 485 and 535 nm, respectively.

#### 2.6 Statistical analysis

Graph pad prism 6 and MS Excel was used for statistical analysis. All experiments were done three times (n=5). The results of each assay are expressed as mean  $\pm$  standard deviation. Differences between

groups were assessed by one-way ANOVA; Statistical significance was accepted at  $p < 0.05$  or 0.001.

### 3. Results

#### 3.1 Characterization of DEP

The DEP was suspended in distilled water, sonicated for 25mins and analyzed by Transmission electron microscope. TEM analysis showed the morphology of collected DEP to be of diffused spheres having average nanoparticle size of  $30 \pm 4\text{nm}$  (Figure 2).

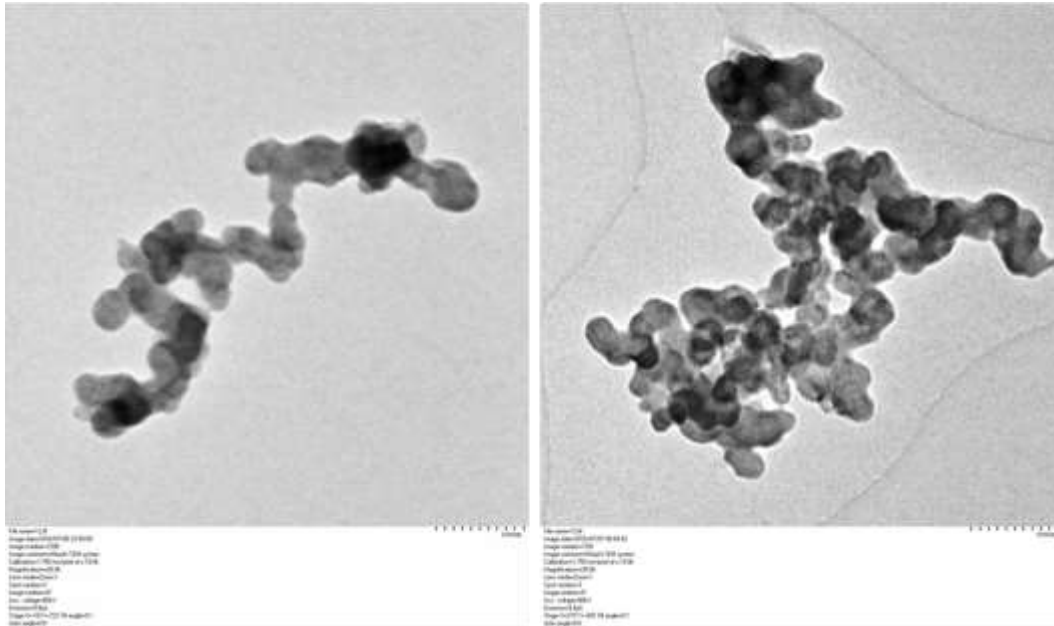


**Figure 2:** Transmission electron micrographs of the DEP collected from diesel engine showed the morphology of the particle to be diffused spheres.

#### 3.2 Diesel exhaust nanoparticles reduce alveolar epithelial barrier integrity

ECIS was used to study the changes in epithelial morphology on challenge with varying concentrations of DEP by sensing the variations in

impedance/resistance offered by A549 monolayer to an AC at 4000Hz. ECIS, the non-invasive biophysical approach showed a drop in impedance on exposure to DEP in a dose-dependent manner (Figure 3).

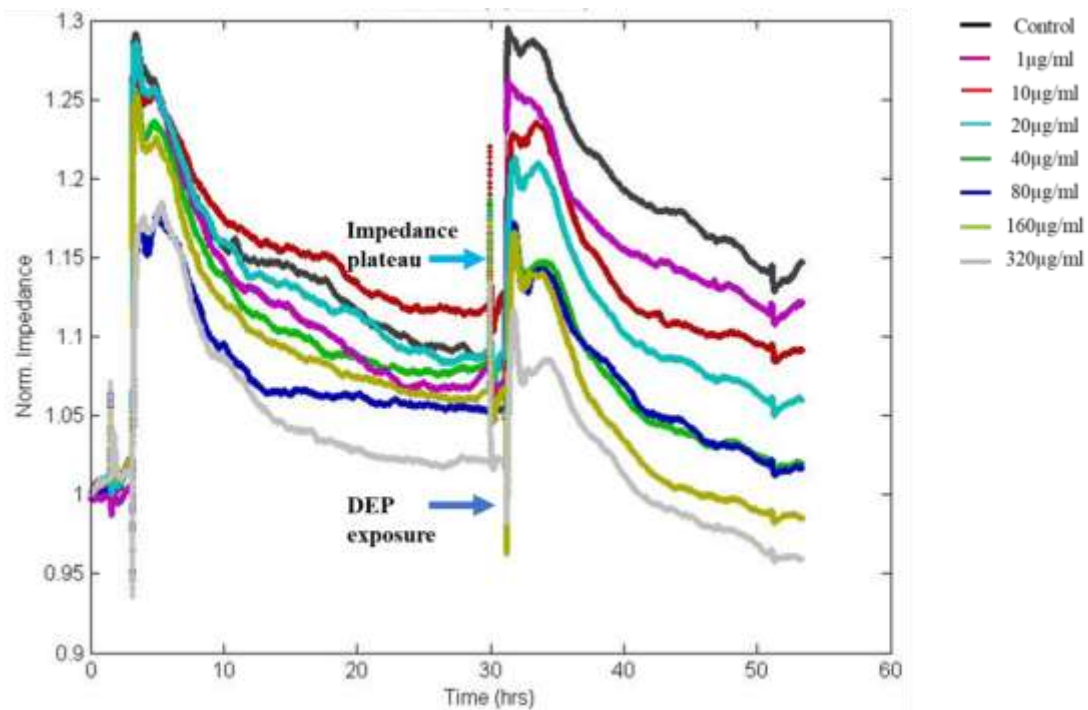


**Figure 3:** The Normalized impedance v/s time graph of ECIS shows a drop in resistance on exposure to DEP, which was dose-dependent. Impedance after 24hrs of DEP exposure showed values nearly equivalent to initial seeding indicating loss of cell-cell adhesion via intercellular junctional proteins and disruption of the monolayer with loss of barrier integrity at high doses. Colour palettes represent the doses of exposure.

In this study, fluctuations in the electrical properties of cell-covered microelectrodes reflected dynamic changes in cell morphology resulting from disrupted cell monolayers following exposure to DEP. The resistance value reached as low as initial seeding resistance 950Ω for the highest dose of DEP after 24hrs of exposure whereas the resistance of untreated control wells reached more than 1200Ω. Decreased

resistance to current flow indicates loss of cell-cell adhesion via intercellular junctional proteins and the disruption of the monolayer with loss of barrier integrity. The impedance was converted into its components, resistance (Figure 4) and capacitance (Figure 5). We observed dose and time-dependent reduction in barrier integrity post-exposure.

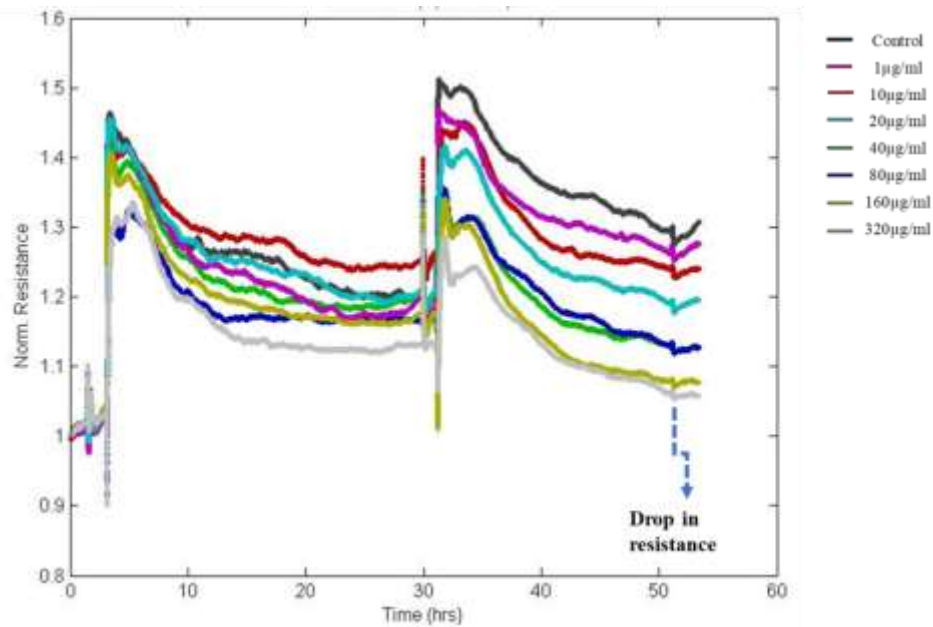


**Figure 4:** The Normalized resistance of DEP exposed A549 cells. Resistance is decreasing in a dose and time-dependent manner after the exposure to DEP indicating a reduction in resistance to current flow through the junctions.

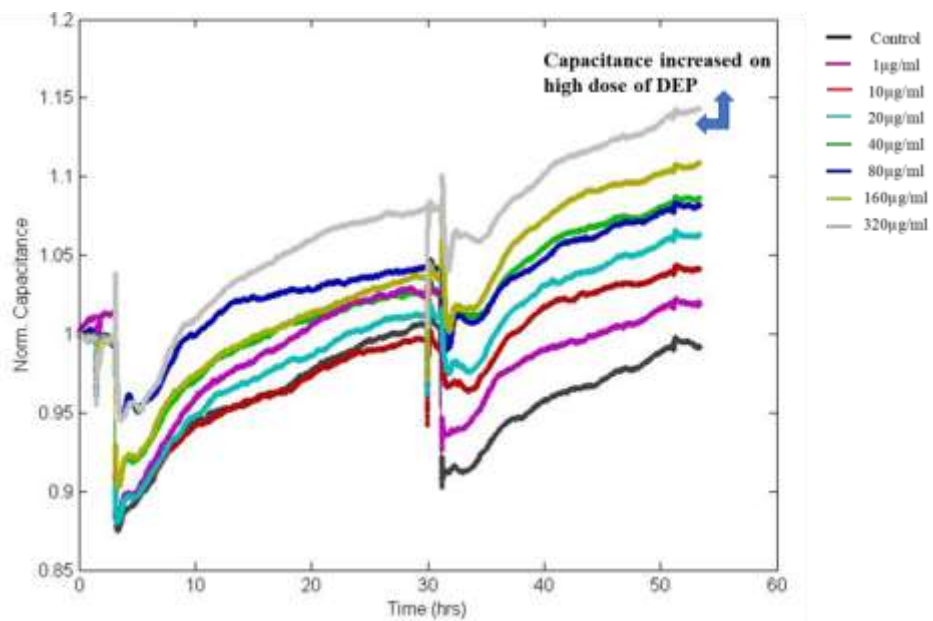


**Figure 5:** Shows Normalized Capacitance to DEP exposed A549 cells. Capacitance is increasing in a dose and time-dependent manner after the exposure DEP.

**3.3 Classical cytotoxicity analyses**

**3.3.1 Exposure to DEP induced a dose-dependent reduction in cell viability:**

The viability of A549 was measured by MTT assay after exposure to different concentrations of DEP for 24hrs (Figure 6a). A dose-dependent reduction in viability was observed after

exposure. The lowest concentration of 1 µg/ml was not cytotoxic. More than 50% loss of viability was observed when cells were exposed to 40 µg/ml DEP. 23.05% viability was observed in the highest dose (320µg/ml) exposure.

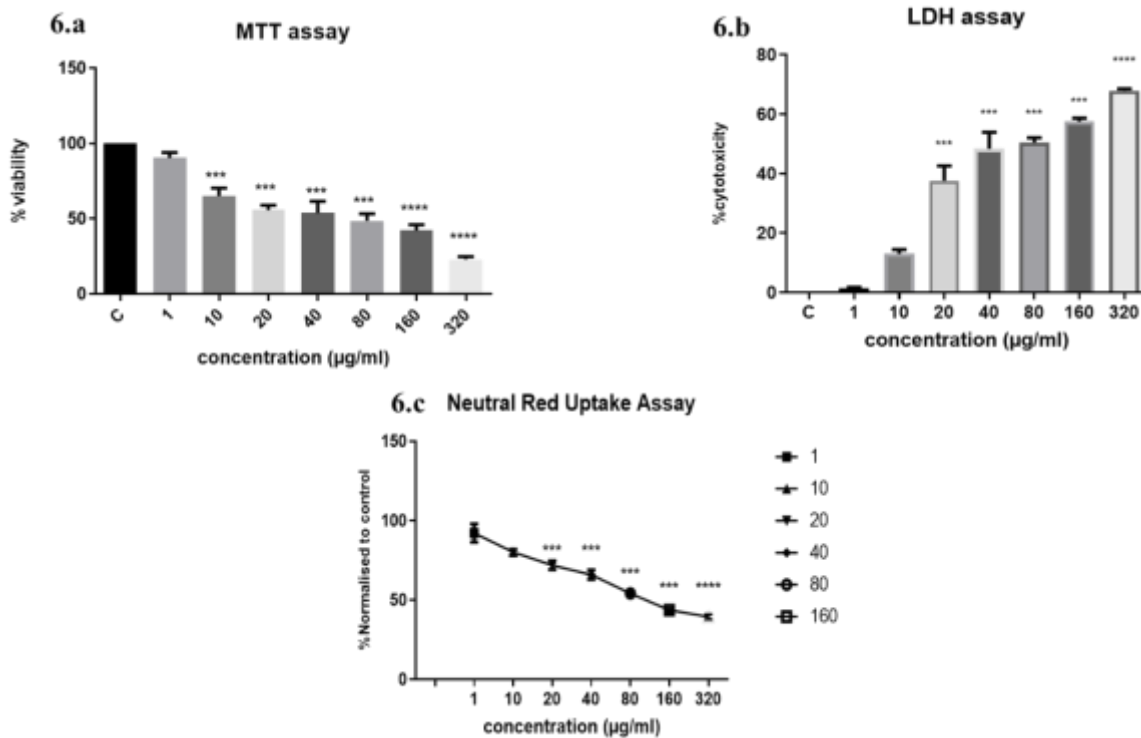


**Figure 6:** Classic endpoint cytotoxicity analyses. (6a) MTT assay of A549 cells exposed to DEP implied a dose-dependent increase in cytotoxicity; (6b) LDH cytotoxicity assay on DEP exposure. The substrate to LDH enzyme was added to culture media of A549 grown in 96 well plates after exposure to DEP. Complete lysis of A549 cells with lysis solution provided max. LDH released to the supernatant. Percentage cytotoxicity was calculated as a ratio of experimental absorbance/ Max. LDH release x 100; (6c) Neutral Red retention in DEP exposed cells. At the higher concentrations which proved to be cytotoxic, lysosome integrity was affected and less than 30% of cells were retaining the dye. The results are expressed as the mean ±SD of 3 independent experiments. \*\*\*p<0.001, \*\*\*\*p<0.0001 were found to be significant. Control wells were not treated with DEP.

**3.3.2 Higher concentrations of DEP reduced the plasma membrane integrity:**

Lactate dehydrogenase is a stable cytosolic enzyme released into the culture medium only on the damage of the plasma membrane.

In the presence of diaphorase enzyme, released LDH from damaged cells could be measured by supplying lactate, NAD<sup>+</sup> and INT as substrates. The generation of a red formazan product is proportional to the amount of LDH released and thereby the number of lysed cells. We observed a significant increase in LDH release at doses of 40 ug and above of DEP. Loss of plasma membrane integrity is indicative of cell death. At 20µg/ml concentration 40% cytotoxicity was observed and more than 50% cytotoxicity was observed above 40ug doses indicating that increasing concentrations were increasingly cytotoxic (Figure 6b).

**3.3.3 DEP exposure induces lysosomal disruption in alveolar epithelial cells:**

The neutral red uptake assay uses the weak cationic dye neutral red (3-amino-7-dimethylamino-2-methylphenazine hydrochloride), which is preferentially absorbed into lysosomes. Intact lysosomal processes are only maintained in viable cells, so the degree of reduction of viability on a challenge with the test compounds indicates the toxicity of the test substance. The retention of the dye was found to be dose-dependent (Figure 6c). At higher concentrations, DEP is cytotoxic and causes lysosomal destabilization.

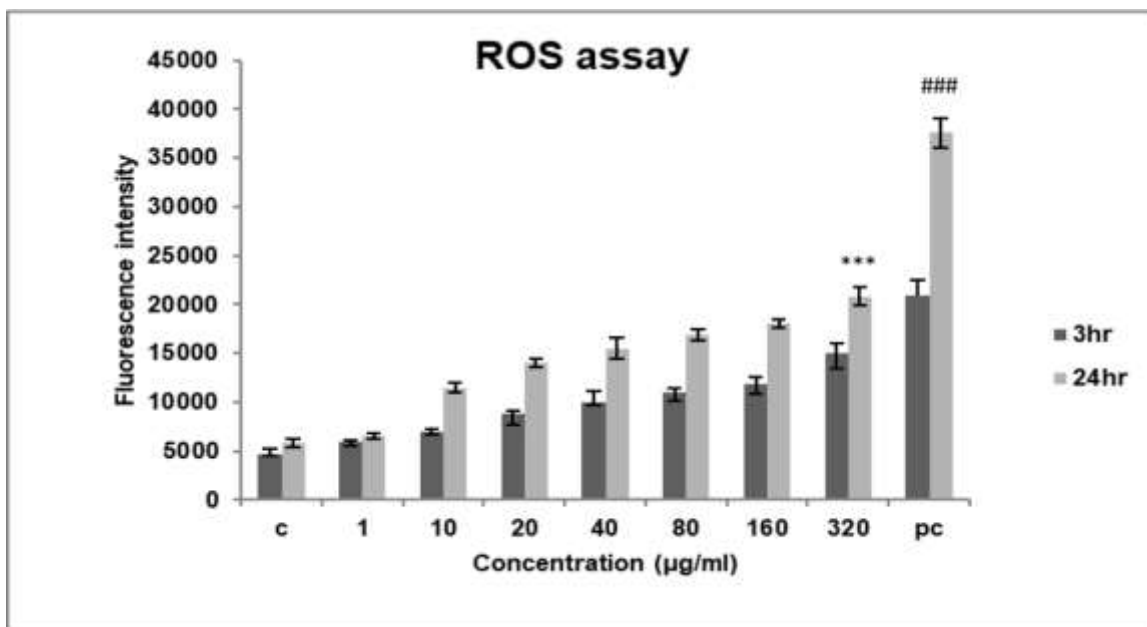


**Figure 7:** Represents ROS measurement of A549 cells exposed to DEP at varying concentrations and time points. The assay showed an increase in ROS production in a dose and time-dependent manner. The results are expressed as the mean ±SD of 3 independent experiments. \*\*\*p<0.001 against control, (###p<0.001 against 3hr) found to be significant.

### **3.4 DEP induces ROS production in alveolar epithelial cells**

To determine the mechanism of cytotoxicity of DEP we assessed intracellular ROS production in A549 cells with a fluorescence probe DCFHDA. Since ROS production is an early response to any cellular insult, we assessed ROS production at two different time points 3hrs and 24hrs.

After exposure to DEP, we found that ROS production increased in a dose and time-dependent manner (Figure 7) in each group. The fluorescent intensity increased by nearly 20000RFU after 24hrs at high concentrations of exposure to DEP.

## **4. Discussion**

We have utilized the real-time, non – destructive label-free ECIS method to understand cellular behaviour to external stimuli or injury. Here the epithelial barrier integrity was assessed on DEP exposure. Epithelial cells form monolayers with tight junctional proteins forming an intact barrier to prevent agents from entering circulation. Our study demonstrates that exposure to DEP can reduce the epithelial barrier integrity in a dose-dependent manner. The label-free, continuous measurements obtained in real-time with the Electrical cell-substrate Impedance Sensing (ECIS), outranks traditional label-based methods for cellular assays. The ECIS system is a convenient, rapid, and highly sensitive tool to non-destructively monitor cellular behaviour by analyzing the cell-substrate impedance, which is determined by cellular morphology and distribution on the sensing electrode [8]. The method can be effectively utilized for studies evaluating the effect of particles in barrier integrity and is an effective tool for high throughput

toxicity assays. The advantage of this technique is the frequent and repeated measurements of electrical resistance, allowing for the assessment of rapid changes in barrier function. A stimulus that induces rapid disruption followed by recovery may be missed using methods that use a single time point assessment which rely on transcellular passage of molecules like dextrans that can be detected at discrete time points. On the other hand using ECIS method, the electrical resistance is a continuous variable measured in real-time simultaneously along with the stimuli and allows for more precise quantification of barrier disruption [9]. The cytotoxic effects of superparamagnetic iron oxide nanoparticles (SPION) on endothelial cells was investigated using ECIS [10]. Despite the active use of SPION in biomedicine and MRI diagnostics due to its low cytotoxicity, ECIS analysis demonstrated a decrease in cell impedance depending on the concentration of nanoparticles used for treatment, resulting in adverse effects on endothelial integrity, a fact that could be used in defining safe strategies or protocols for clinical application. Likewise, even the slightest morphological variation in adherent cells could be assessed in terms of change in resistance by ECIS. We observed a dose-dependent drop in resistance measurements and the values even reached the range of initial seeding i.e complete absence of adherent cells on exposure at a high dose. This implied a loss in barrier integrity upon DEP exposure at high doses.

Caraballo et al demonstrated that DEP induced transepithelial conductance, loosening of tight junction in alveolar epithelial cells [11]. Lehman et al., also observed disruption of occludin arrangement in epithelial cells when exposed to the high dose of

DEP (125 µg/ml) [12]. These findings suggested that DEP can induce structural changes [13] but they have used standard reference material (NIST) for exposure, which they considered as a surrogate for fresh DEP. Also, they have utilized FITC-Dextran labelling and ERS milli cell volt-ohmmeter to study barrier integrity which has all the limitations mentioned earlier.

We compared our results with classic endpoint cytotoxicity methods like MTT and LDH. The endpoint results were comparable but these results take longer to manifest whereas in ECIS cytotoxicity could be estimated in real time and early on. Lysosomes formally considered as cellular incinerators have now emerged as critical sites for plasma membrane repair, signaling and energy metabolism [14]. Lysosomes also participate in the digestion of endocytosed and autophagocytosed material and are involved in maintaining intracellular Ca<sup>2+</sup> homeostasis [15]. Nanomaterials entering the endo-lysosomal system can lead to dysfunction of lysosomes which in turn leads to several diseases [16, 17]. Previous studies with TiO<sub>2</sub> reported lysosomal destabilization as a cytotoxicity mechanism in human bronchial epithelial cells and murine fibroblast cells [18, 19]. Our results also show that DEP induces loss of lysosomal integrity and the destabilization is dose-dependent, as indicated by the Neutral red uptake (NRU) assay results. The NRU assay relies upon the weakly cationic vital dye neutral red (NR) uptake, which accumulates in the lysosomes and endosomes of living cells, but not in dead or dying cells, by non-ionic passive diffusion [20, 21]. The quantity of dye retention by the cells is assumed to be proportional to the total number of viable cells present [22]. We

observed a dose-dependent reduction in dye retention indicative of loss of lysosome integrity and its destabilization. Cudazzo et al., reported a reduction in NRU as an indication of the lysosomotropic potential of E-cigarettes [23]. They reported nicotine-induced changes in the acidic compartments of multiple mammalian cell lines. Our observations also point to a reduction in dye retention which could be attributed to changes in the acidic compartments. A previous study had indicated that the disruption of epithelial tight junctions and the resulting loss of barrier function play a crucial role in the pathogenesis of a variety of gastrointestinal, hepatic, pulmonary, kidney and ocular diseases, so it is imperative that the barrier function be analysed in real-time to get a realistic idea of cytotoxicity.

We assessed the possible mechanism of cytotoxicity induction also. Increased ROS production disrupts the epithelial and endothelial barrier function by destabilizing tight junctions [24]. The delicate balance between the rate and amount of ROS production and the rate of oxidant elimination maintains normal cellular homeostasis. When the production of ROS overwhelms the cellular antioxidant capacity, the result will be “Oxidative stress”. ROS are generally cleared from the cell by the action of catalase, superoxide dismutase (SOD) or glutathione (GSH) peroxidase. Overproduction of ROS damages cells by altering macromolecules such as polyunsaturated fatty acids in membrane lipids, protein denaturation, and ultimately DNA. Oxidative stress, induced by various reactive oxygen species such as hydrogen peroxide, nitric oxide, peroxynitrite and hypochlorous acid is known to disrupt epithelial and endothelial tight junctions. The mechanisms involved in the oxidative

stress-induced disruption of tight junction include protein modification such as thiol oxidation, phosphorylation, nitration and carbonylation. In our study we assessed ROS production in line with the increased cytotoxic responses and observed a dose and time-dependent increase in ROS production.

## 5. Conclusion

The present study illustrates that Diesel exhaust nanoparticles collected directly from vehicle emission induce loss of barrier integrity and cytotoxicity in a dose-dependent manner. The likely mechanism of DEP mediated cytotoxicity could be the formation of intracellular ROS and changes in acidic compartments of lysosomes.

Our study clearly shows that ECIS will be a simple, high throughput, valuable tool in understanding the effects of external stimuli on cell monolayers vis-à-vis labour-intensive endpoint analyses, proving to be an easy tool for cytotoxicity assays. It is to be noted that ECIS provided more sensitive results compared to other assays.

## Acknowledgement

The authors thank Director SCTIMST & Head BMT wing for providing infrastructure to carry out the study, DST INSPIRE for fellowship and DBT for funding part of the project.

## Conflict of Interest

The authors declare that they have no conflict of interest and no affiliation with or involvement in any organization or entity with any financial interest related to this study.

## References

1. Giaever I, Keese CR. Monitoring fibroblast behavior in tissue culture with an applied electric field. *Proc Natl Acad Sci USA* (1984) : 3761-3764.
2. Gauderman WJ, et al. Childhood asthma and exposure to traffic and nitrogen dioxide. *Epidemiology* (2005): 737-43.
3. Laden F, et al. Reduction in fine particulate air pollution and mortality: extended follow-up of the Harvard six cities study. *Am J Respir Crit Care Med* (2006): 667-72.
4. Wichmann HE. Diesel exhaust particles. *Inhal Toxicol* 19 (2007): 241-244.
5. Szulcek R, Bogaard HJ, van Nieuw Amerongen GP. Electric cell-substrate impedance sensing for the quantification of endothelial proliferation, barrier function, and motility. *J Vis Exp* 28 (2014): 51300.
6. Borenfreund E, Puerner JA. Toxicity determined in vitro by morphological alterations and neutral red absorption. *Toxicol Lett* (1985): 119-124.
7. Ngoc Le HT, Kim J, Park J, et al. A Review of Electrical Impedance Characterization of Cells for Label-Free and Real-Time Assays. *BioChip J* (2019): 295-305.
8. Suresh K, Servinsky L, Johnston L, et al. Comparison of polynomial fitting versus single time point analysis of ECIS data for barrier assessment. *Physiological reports* 9 (2021): e14983.
9. Astanina, Ksenia, Simon, et al. Superparamagnetic iron oxide nanoparticles impair endothelial integrity and inhibit nitric

- oxide production. *Acta Biomaterialia* (2014): 4896-4911.
10. Caraballo JC, Ishii C, Westphal W, et al. Ambient particulate matter affects occludin distribution and increases alveolar transepithelial electrical conductance. *Respirology* (2011): 340-349.
  11. Lehmann AD, Blank F, Baum O, et al. Rothen-Rutishauser: Diesel exhaust particles modulate the tight junction protein occludin in lung cells in vitro. *Particle and Fibre Toxicology* 6 (2009).
  12. Schwarze PE, Totlandsdal AI, Låg M, et al. Inflammation-related effects of diesel engine exhaust particles: studies on lung cells in vitro. *Biomed Res Int* (2013): 685142.
  13. Settembre C, Fraldi A, Medina DL, et al. Signals from the lysosome: a control centre for cellular clearance and energy metabolism. *Nat Rev Mol Cell Biol* (2013): 283-296.
  14. Brini M, Calì T, Ottolini D, et al. Intracellular calcium homeostasis and signaling. In *Metallomics and the Cell*; Springer (2013): 119-168.
  15. Platt FM, Boland B, vander Spoel AC. Lysosomal storage disorders: The cellular impact of lysosomal dysfunction. *J. Cell Biol* (2012): 723-734.
  16. Kong H, Xia K, Pan L, et al. Autophagy and lysosomal dysfunction: A new insight into mechanism of synergistic pulmonary toxicity of carbon black-metal ions co-exposure. *Carbon* (2017): 322-333.
  17. Jin C, Zhu B, Wang X, et al. Cytotoxicity of Titanium Dioxide Nanoparticles in Mouse Fibroblast Cells Cytotoxicity of Titanium Dioxide Nanoparticles in Mouse Fibroblast. *Chem. Res. Toxicol* (2008): 1871-1877.
  18. Hussain S, Thomassen LCJ, Ferecatu I, et al. Carbon black and titanium dioxide nanoparticles elicit distinct apoptotic pathways in bronchial epithelial cells. *Part. Fibre Toxicol* (2010): 1-17.
  19. Winckler J. Vitalfärbung von Lysosomen und anderen Zellorganellen der Ratte mit Neutralrot [Vital staining of lysosomes and other cell organelles of the rat with neutral red (author's transl)]. *Prog Histochem Cytochem* 6 (1974): 1-91.
  20. Filman DJ, Brawn RJ, Dandliker WB. Intracellular supravital stain delocalization as an assay for antibody-dependent complement-mediated cell damage, *Journal of Immunological Methods* (1975): 189-207.
  21. Repetto G, del Peso A, Zurita J. Neutral red uptake assay for the estimation of cell viability/cytotoxicity. *Nat Protoc* 3 (2008): 1125-1131.
  22. Cudazzo, Gianluca, Smart, et al. Lysosomotropic-related limitations of the BALB/c 3T3 cell-based neutral red uptake assay and an alternative testing approach for assessing e-liquid cytotoxicity. *Toxicology in Vitro* (2019): 104647.
  23. Radhakrishna Rao Oxidative stress-induced disruption of epithelial and endothelial tight junction *Frontiers in Bioscience* (2008): 7210-7226

24. Hellowell B, Gutteridge JMC. Free radicals in biology and medicine. Oxford: Oxford

Univ Pr (1999).



This article is an open access article distributed under the terms and conditions of the [Creative Commons Attribution \(CC-BY\) license 4.0](https://creativecommons.org/licenses/by/4.0/)